Proceedings of the
Annual Stability Conference
Structural Stability Research Council
San Antonio, Texas, March 21-24, 2017

Cold-Formed Steel Beam-Columns: Experimental Program, Numerical Analyses, Design Code Development, and Design Tools

Shahabeddin Torabian[1] and Benjamin W. Schafer[2]

Abstract
This paper summarizes the newly proposed Direct Strength Method (DSM) for cold-formed steel beam-columns and introduces the developed design code and design tools. DSM is a robust and flexible design method available in the AISI Specification (AISI -S100) for designing thin-walled steel beams and columns. Currently, no explicit method is available in the Specification for designing under combined actions, as beam-columns are designed using linear interaction equations. As a result, the cross-section stability analyses are performed only under two simplistic stress distributions: i.e., stress due to isolated compression and bending. This study provides an integrated, explicit design method for beam-columns that uses new design expressions but still encompasses the current DSM method for isolated beams and columns. The new beam-column DSM has recently been validated against the results of an experimental program on lipped channels and Zee-sections. Further, nonlinear geometric and material collapse analyses have been performed on the tested specimens to establish a modeling protocol for cold-formed steel beam-columns. Parametric studies using the modeling protocols have been leveraged to validate the proposed DSM for a wide variety of cross-sections. To ease implementation of the new method, CUFSM (a finite strip method program for elastic buckling analyses) has been recently improved to incorporate the generalized definition of the combined actions in the stability analysis and also to provide yield and plastic strength surfaces, which are essential in the new DSM beam-column implementation. The proposed method has the potential to provide a more mechanically sound solution to the strength of beam-columns, increase performance, and enable a new generation of optimized and high strength cold-formed steel shapes across a variety of loading actions.

1. Introduction

In current cold-formed steel design specifications such as AISI S100 or AS/NZS 4600, combined actions on a member are taken into account through a simple linear combination of pure axial or flexural strength previously determined using the Effective Width Method (EWM) or the Direct Strength Method (DSM) (AISI 2016; Standards Australia 2005).

[1] Associate Research Scientist, Dept. of Civil Engineering, Johns Hopkins University <torabian@jhu.edu>
[2] Professor, Dept. of Civil Engineering, Johns Hopkins University, <schafer@jhu.edu>

Although extensive efforts have been devoted to estimating the capacity of cold-formed steel members under pure axial or flexural actions (see reviews by Hancock 2003; Macdonald et al. 2008; Rondal 2000; Schafer 2008; Young 2008), the design of structural members under explicit combined actions has been rarely studied in either EWM or DSM (Kalyanaraman and Jayabalan 1994; Loh 1985; Miller and Pekoz 1994; Pekoz 1986; Peterman 2012; Shifferaw 2010).

This study provides an integrated, explicit design method for beam-columns that uses new design expressions but still incorporates the current DSM method for isolated beams and columns. The development of the DSM beam-column design method is summarized as follows. First, a formal definition of the P-M_1-M_2 beam-column space is provided. Next, experimental studies on the lipped channel and Zee-shaped beam-columns are briefly explained. Then, the numerical analyses and parametric studies are described. This is followed by a brief description of the new DSM expressions for beam-columns. Finally, the paper concludes by comparing the proposed DSM beam-column method against available test results and introducing the design tools facilitating the implementation of the proposed DSM beam-column strength prediction method.

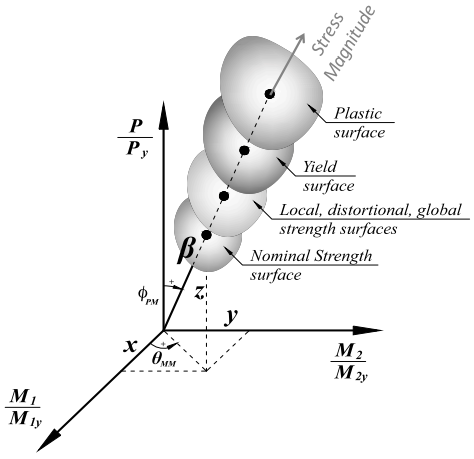

Figure 1: Normalized P-M_1-M_2 space and conceptual plastic, yield, and strength surfaces.

2. Generalized P-M_1-M_2 space and β, θ_{MM}, ϕ_{PM} coordinate system

A normalized P-M_1-M_2 space is utilized to define the state of the combined actions including bi-axial bending moments about principal axes (M_1, M_2) and axial load (P) normalized with respect to the corresponding first yield strength (M_{1y}, M_{2y}, and P_y). The coordinates in the P-M_1-M_2 space are defined as:

$$x = \frac{M_1}{M_{1y}},\ y = \frac{M_2}{M_{2y}},\ z = \frac{P}{P_y} \tag{1}$$

where M_1 is defined as the major principal axis of bending, and M_2 as the minor principal axis of bending. Points in the normalized P-M_1-M_2 space are defined by an azimuth angle, θ_{MM}, an elevation angle, ϕ_{PM}, and a radial length β, as follows,

$$\theta_{MM} = \tan^{-1}(y/x)$$
$$\phi_{PM} = \cos^{-1}(z/\beta) \quad (2)$$
$$\beta = \sqrt{x^2 + y^2 + z^2}$$

For any θ_{MM} and ϕ_{PM}, the elastic stress distribution on a given cross-section can be determined; β is still required to know the absolute magnitude, as shown in Fig. 1.

3. Experimental Program

The failure modes and ultimate capacity of fifty-five 600S137-54 (AISI S200-12 nomenclature) lipped channel and forty-three 700S225-60 (similar to AISI S200-12 nomenclature) Zee-section beam-columns under combined bi-axial bending moments and axial load have been previously characterized by the authors in a experimental program specifically planned to explore beam-column behavior (Torabian et al. 2015, 2016c; b). Fig. 1 shows the test rig applying combined axial load and bending moment via eccentric loading. The lipped channel specimens were three different lengths: 305 mm (short), 610 mm (intermediate), and 1219 mm (long), and the Zee-section specimens were 305 mm and 1219 mm in length. The mean test-to-predicted ratio for the 98 specimens using DSM as implemented in AISI S100-16 with a linear interaction beam column expression was 1.40 with a coefficient of variation (C.o.V) of 19.8% and for EWM the mean was 1.36 with a C.o.V of 22.4%. See Torabian et al. (2015, 2016b; a) for complete details.

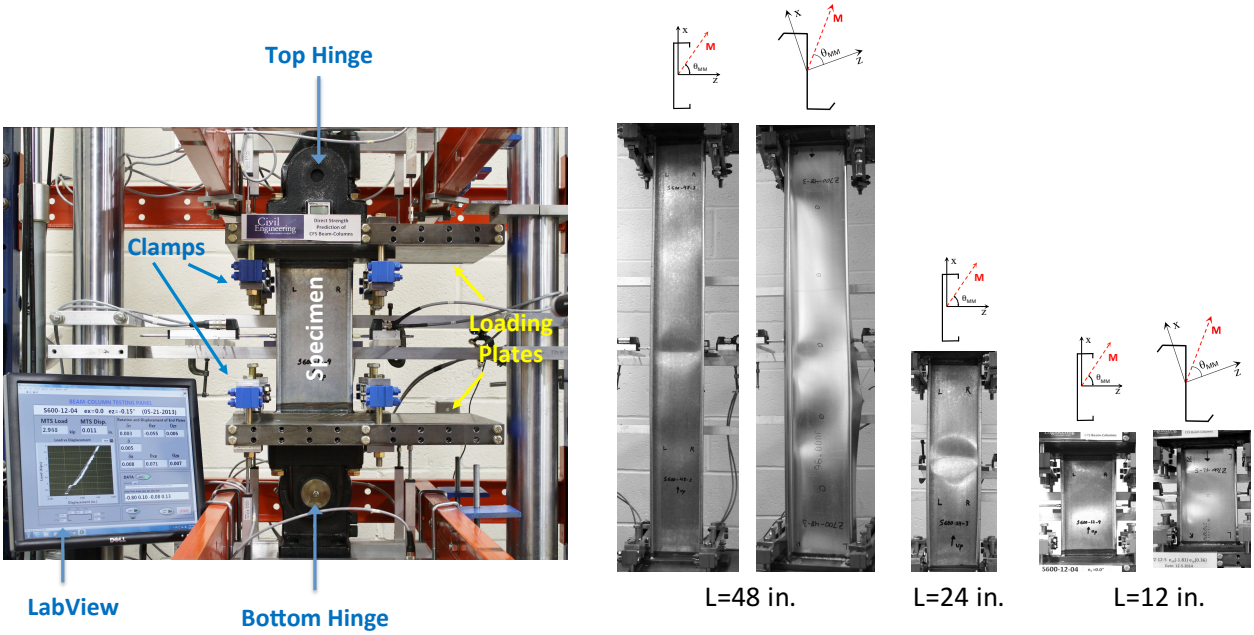

Figure 2: Beam-column test rig; and lipped channel and Zee-section test specimens.

4. Numerical Analyses

Cold-formed steel lipped channels and Zee-sections under combined axial force and biaxial bending moments have been explored by geometric and material nonlinear shell finite element collapse analyses performed in ABAQUS and the modeling protocols are validated by the experimental results discussed in Section 3.

4.1 Modeling Protocols

The modeling protocols include boundary conditions, geometrical modeling, element type, mesh details, residual stresses and strains, and geometric imperfections. For both lipped channels and Zee-Sections, quadratic quadrilateral 9-node S9R5 shell elements have been used: 10 elements in the web, 2 elements in the flange and the lip, and 4 elements in the corner. The mesh aspect ratio is kept near one. The von Mises yield criteria, associated flow, and isotropic hardening were assumed for modeling plasticity. For defining material properties, true stress-strain properties based on coupon tests have been used. Roll-forming effects have been considered only for the corners base on the method set forth by Moen et al. (2008) and residual stresses and strains assigned to 31 integration points through the thickness. Notably, residual stresses and strains turned out to have only small effects on the strength. Measured geometric dimensions (when available) have been implemented in the modeling. The imperfection pattern consisted of two sympathetic local and distortional modes along with global modes. Lipped channels are less sensitive to the sign of the imperfection pattern; however, the outward flange deformation in distortional buckling provides the most conservative results. In Zee-sections, imperfections that provide inward distortional deformation in the compressive flange provides more realistic results. For lipped channels, the imperfection magnitude of 50%ile from Zeinoddini and Schafer (2012) provided the most consistent results. However, for Zee-sections it was found that an imperfection magnitude of 95%ile from Zeinoddini and Schafer (2012) was in better agreement with the results. Imperfection magnitudes were also measured for comparison in Zhao et al. (2015) For more details see (Torabian et al. 2014a, 2016a; c).

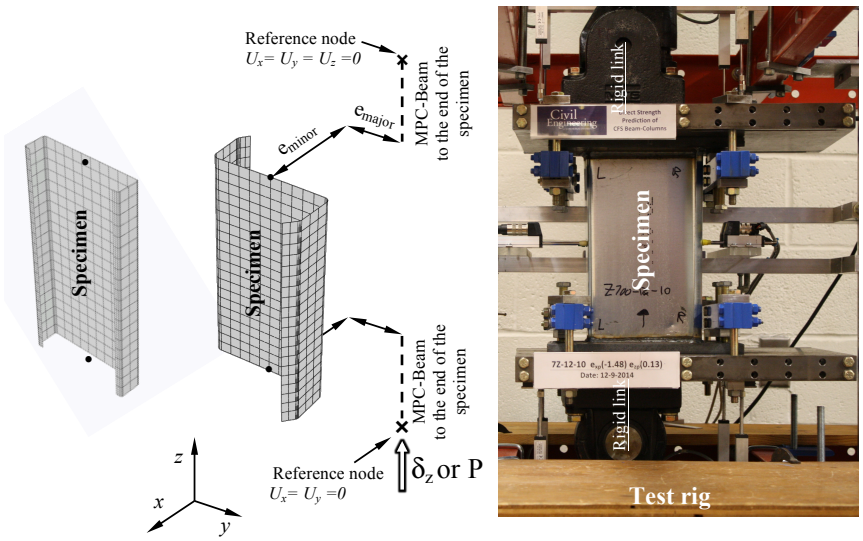

Figure 3: Numerical modelling: geometry and mesh of the models, boundary conditions, and constrains.

4.2 Parametric Studies

Using the proposed modeling protocols, the strength of more cross-sections (see Fig. 2) under more combinations of axial load and bending moments can be determined and the results can be used to evaluate the newly proposed DSM method for beam-column as discussed in (Torabian et al. 2014b)

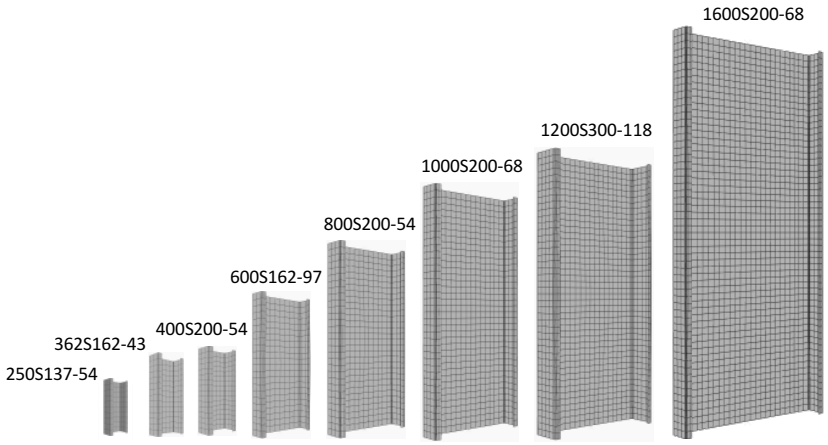

Figure 4: Parametric analysis on different sizes of the lipped channel beam-columns

5. Design Code Development

A generalized DSM for beam-column was sought that provides the strength of cold-formed steel beam-columns under an arbitrary longitudinal stress distribution using the generalized β, θ_{MM}, ϕ_{PM} coordinate system. The yield and stability limits may be characterized in terms of β magnitudes along the θ_{MM}, ϕ_{PM} angles, i.e. β_y and β_p for yielding and plastic behavior, and β_{crG}, β_{crD}, and β_{crL} for global, distortional, and local elastic buckling, respectively.

5.1 Yield and Plastic Strength (β_y and β_p)

The first yield and fully plastic behavior of a lipped channel (600S137-54) is shown in the P-M_1, P-M_2, and M_1-M_2 space in Fig. 5. A lipped channel beam-column under axial load and minor axis bending (P-M_2) has significantly greater elastic and plastic capacity than the linear interaction expression. This shows how considering actual stress distribution can help in optimizing the strength prediction of cold-formed steel members.

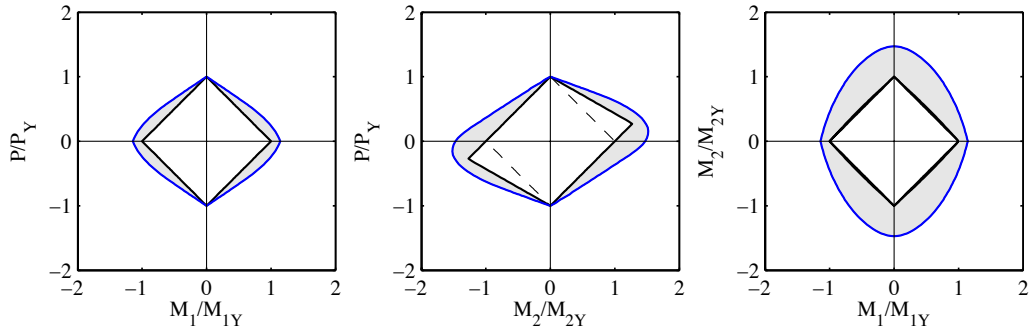

Figure 5: First yield (solid black line) and plastic strength (solid blue line) of fully effective sections, and linear interaction equation (dashed line). The lipped channel is 600S137-54.

5.2 Elastic Buckling Response (β_{crG}, β_{crL}, and β_{crD})

For an arbitrary loading condition, the reference stress corresponding to the yield surface (β_y, θ_{MM}, ϕ_{PM}), where the maximum stress is F_y, can be determined. Performing stability analysis under this stress distribution will directly result in normalized buckling factors: β_{crG}/β_y, β_{crL}/β_y,

and β_{crD}/β_y for global, local, and distortional buckling, respectively, as shown in Fig. 6. This process has been automated in the latest version of CUFSM (Schafer and Adany 2006) as discussed in Section 6.

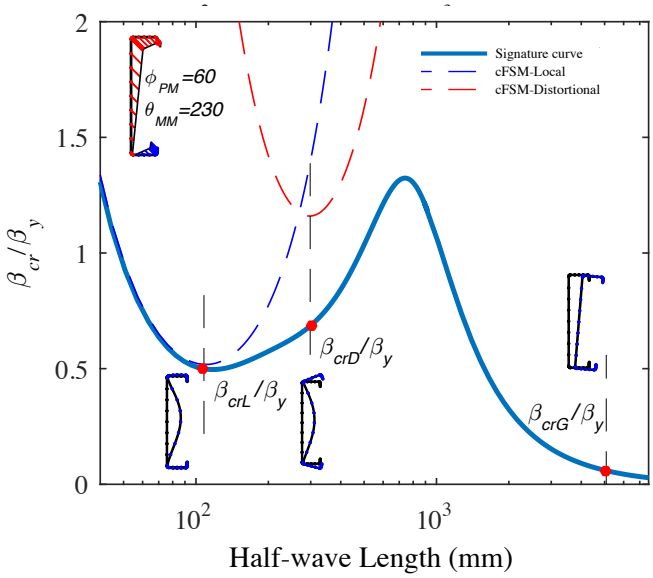

Figure 6: Semi-analytical finite strip method signature curves for 600S137-54 lipped channel under a generalized applied action. Elastic buckling β_{crG}, β_{crL}, and β_{crD} are direct generalizations of the combined axial load and bending moment actions.

Global, local, and distortional elastic buckling surfaces in the P-M_1, P-M_2, and M_1-M_2 space are shown in Fig. 7. The stability of the member is highly nonlinear and a linear representation is not a viable approximation.

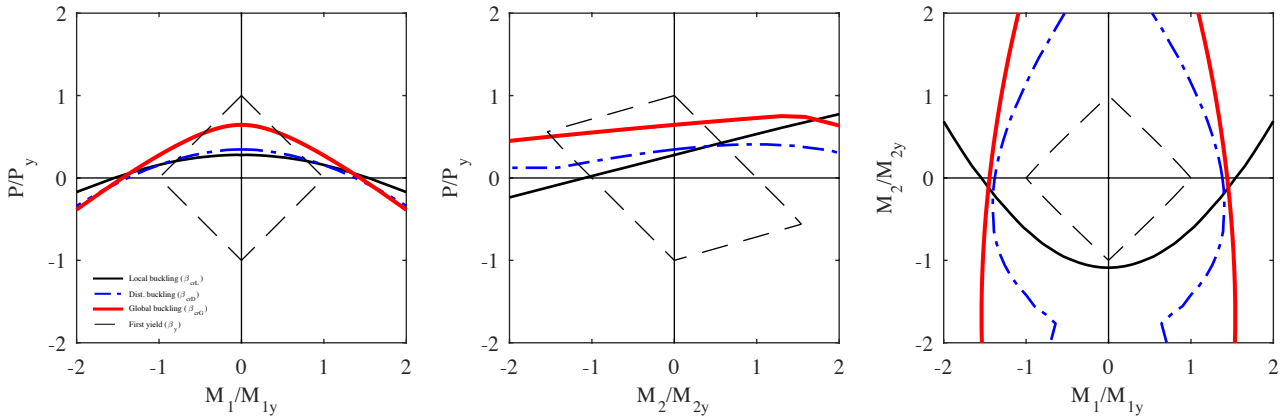

Figure 7: Global (solid red line), local (black solid line), and distortional (dash-dot blue line) elastic buckling, , yield (dashed black thin line) curves for 600S137-54, L= 914 mm.

5.3 Proposed Beam-Column DSM

5.3.1. Global Buckling (β_{nG})

The DSM expressions for nominal global buckling strength (β_{nG}) of beam-columns under combined axial load and bending is as follows (for more detailed expressions see Torabian et al. (2016c)):

$$\beta_{nG} = \beta_{nGP} + (\beta_{nGM} - \beta_{nGP}) \sin\phi_{PM} \tag{3}$$

where β_{nGP} (global strength as a column) and β_{nGM} (global strength as a beam) are as follows,

$$\beta_{nGP} = \begin{cases} 0.658^{\lambda_G^2}\beta_y & \lambda_G \le 1.5 \\ 0.877\lambda_G^{-2}\beta_y & \lambda_G > 1.5 \end{cases}, \text{ where } \lambda_G = \sqrt{\frac{\beta_y}{\beta_{crG}}} \tag{4}$$

$$\beta_{nGM} = \begin{cases} \beta_P - \left(\beta_P - \beta_y\right)\dfrac{\lambda_G - 0.23}{0.37}\beta_y & \lambda_G \le 0.6 \\ \dfrac{10}{9}\left(1 - \dfrac{10}{36}\lambda_G^2\right)\beta_y & 0.6 \le \lambda_G \le 1.336 \\ \lambda_G^{-2}\beta_y & \lambda_G > 1.5 \end{cases} \tag{5}$$

5.3.2. Local Buckling (β_{nL})

Local-global interaction is adopted in the proposed beam-column DSM. The nominal capacity of beam-columns in local buckling, β_{nL}, can be determined as a function of local slenderness λ_L, defined as follows: (for more detailed expressions see Torabian et al. (2016c))

$$\beta_{nL} = \begin{cases} \beta_y + (1 - C_{yL}^{-2})(\beta_p - \beta_y) & \lambda_L \le 0.776 \\ \left(1 - 0.15\lambda_L^{-0.8}\right)\lambda_L^{-0.8}\beta_y & \lambda_L > 0.776 \end{cases}, \ \beta_{nG} > \beta_y$$

$$\beta_{nL} = \begin{cases} \beta_{nG} & \lambda_L \le 0.776 \\ \left(1 - 0.15\lambda_L^{-0.8}\right)\lambda_L^{-0.8}\beta_{nG} & \lambda_L > 0.776 \end{cases}, \ \beta_{nG} \le \beta_y \tag{6}$$

$$\text{where } \begin{cases} \lambda_L = \sqrt{\beta_y / \beta_{crL}} & \beta_{nG} > \beta_y \\ \lambda_L = \sqrt{\beta_{nG} / \beta_{crL}} & \beta_{nG} \le \beta_y \end{cases}$$

5.3.3. Distortional Buckling (β_{nD})

The nominal capacity of beam-columns in distortional buckling, β_{nD}, is determined as a function of distortional slenderness λ_D as follows: (for more detailed expressions see Torabian et al. (2016c))

$$\beta_{nD} = \begin{cases} \beta_y + (1 - C_{yD}^{-2})(\beta_p - \beta_y) & \lambda_D \le 0.561 + 0.112\sin\phi_{PM} \\ \left(1 - c_1\lambda_D^{c_2}\right)\lambda_L^{c_2}\beta_y & \lambda_D > 0.561 + 0.112\sin\phi_{PM} \end{cases}, \text{ where } \lambda_D = \sqrt{\frac{\beta_y}{\beta_{crD}}} \tag{7}$$

$$c_1 = 0.25 - 0.03\sin\phi_{PM}, \ c_2 = 0.2\sin\phi_{PM} - 1.2 \tag{8}$$

5.3.4 Nominal Strength and design check (β_n)

The nominal strength is the minimum of the three limit states, as follows:

$$\beta_n = \min(\beta_{nG}, \beta_{nL}, \beta_{nD}) \tag{9}$$

The design check for LRFD method can be performed as follows,

$$\phi = \phi_P + (\phi_M - \phi_P)\sin\phi_{PM} \tag{10}$$

where $\phi_P=\phi_c=0.85$; or $\phi_P=\phi_t=0.9$, and $\phi_M=\phi_b=0.9$, typically.

$$\phi\beta_n \geq \beta_r \tag{11}$$

or for ASD,

$$\Omega = \Omega_P + (\Omega_M - \Omega_P)\sin\phi_{PM} \tag{12}$$

where $\Omega_p=\Omega_c=1.80$ (for compression, typically) and $\Omega_p=\Omega_t=1.67$ (for tension, typically), and for bending $\Omega_p=\Omega_b=1.67$, typically.

$$\beta_n/\Omega \geq \beta_r \tag{13}$$

See Torabian et al. (2016c) for complete details, including alternatives to the sine term in Eq. (3), (8), (10) and (12) that mixes the column and beam solutions.

5.4 Validation

Table 2 provides a detailed examination of the test-to-predicted ratios (β_{Test}/β_n) for all tested lipped channel and Zee-section specimens. Overall, the mean test-to predicted ratio of 1.16, is significantly improved from current design, but still conservative. The loading condition of axial load and minor axis bending is particularly underestimated by the proposed method, especially in the short specimens where the global buckling capacity is high and the behavior is controlled by local or distortional modes. The inelastic reserve associated with minor axis bending at the anchor points may be too conservative in the AISI design specification, as the inelastic reserve was implemented with a certain degree of built-in conservatism, and may need some additional modifications (Shifferaw 2010; Shifferaw and Schafer 2012; Torabian et al. 2014a) to reach better general agreement.

Table 3: Test-to-predicted ratio (β_{Test}/β_n) statistics for all tested specimens

Specimen identifier		Lipped channel (600S137-54) Length (mm) 305	610	1219		Zee-section (700Z225-60) Length (mm) 305	1219
1	$P+M_2$	1.748 [a]	1.622 [a]	1.240 [a]	$P+M_2$	1.239 [a]	1.071 [a]
2		1.448 [a]	1.334 [a]	1.067 [a]		1.378 [a]	0.866 [a]
3		1.102 [a]	1.095 [a]	0.977 [a]		1.389 [a]	1.022 [a]
4		1.471 [a]	1.276 [a]	0.828 [a]		1.192 [a]	0.957 [e]
5		1.402 [a]	1.152 [a]	0.897 [a]	$P+M_{yy}$	1.342 [e]	0.830 [e]
6		1.388 [a]	1.197 [a]	1.022 [a]		1.318 [e]	0.868 [e]
7	$P+M_1$	1.224 [b]	1.407 [b]	1.258 [b]		1.313 [e]	1.032 [b]
8		1.143 [b]	1.190 [b]	1.207 [b]		1.295 [e]	0.851 [c]
9		1.104 [b]	1.158 [b]	1.163 [b]	$P+M_1$	1.096 [b]	0.752 [b]
10	$P+M_1+M_2$	1.322 [c]	1.432 [c]	1.071 [c]		1.043 [b]	1.077 [b]
11		1.131 [c]	1.245 [c]	1.072 [c]		0.881 [b]	0.883 [f]
12		1.372 [c]	1.347 [c]	0.905 [c]	$P+M_{zz}$	1.080 [f]	0.799 [f]
13		1.307 [c]	1.270 [c]	0.965 [c]		0.963 [f]	1.122 [c]
14		1.196 [c]	1.209 [c]	1.034 [c]		1.158 [c]	0.964 [c]
15		1.369 [c]	1.334 [c]	1.108 [c]		1.109 [c]	1.056 [c]
16		1.273 [c]	1.263 [c]	1.318 [c]		1.344 [c]	1.109 [c]
17		1.215 [c]	1.299 [c]	1.202 [c]	$P+M_1+M_2$	1.346 [c]	0.951 [c]
18	P, $P+M_1$		1.305 [d]	1.110 [d]		1.243 [c]	0.874 [c]
19			1.162 [b]			1.209 [c]	0.908 [c]
20			1.384 [d]			1.188 [c]	0.808 [c]
21						1.009 [c]	1.107 [d]
22					P	1.197 [d]	
mean		1.307	1.284	1.080		1.197	0.948
C.o.V		12.6%	9.4%	12.5%		11.9%	12.2%
Mean (all 98 specimens)		1.159					
C.o.V (all 98 specimens)		16.3%					

[a] Minor axis bending and axial load ($P+M_2$)
[b] Major axis bending and axial loads ($P+M_1$)
[c] Biaxial axis bending and axial load ($P+M_1+M_2$)
[d] Axial load (P)
[e] Minor axis (geometric) bending and axial load ($P+M_{yy}$)
[f] Major axis (geometric) bending and axial load ($P+M_{zz}$)

6. Design Tools

6.1 Generalized Demand Definition (β-θ_{MM}-ϕ_{PM}) and Yield Surface

In the latest version of CUFSM (version 4.5, see Schafer and Adany 2006 for citation to previous version), the generalized demand definition (β-θ_{MM}-ϕ_{PM}) can be directly used to define stress distribution. The stress distribution shown in Fig. 6 has been applied and the corresponding yield point ($\beta_{y\ or}\ Beta_y$) is provided by CUFSM, as shown in Fig. 8.

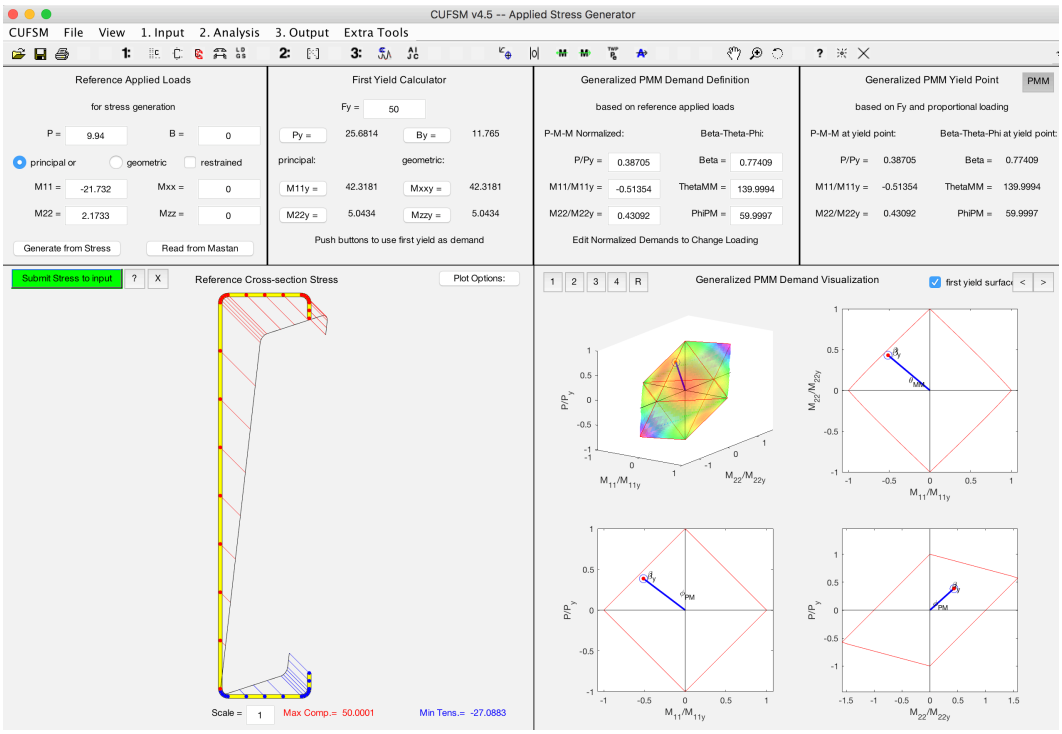

Figure 8: Generalized demand definition interface; and yield surface of a lipped channel cross-section (600S137-54) in CUFSM v4.5.

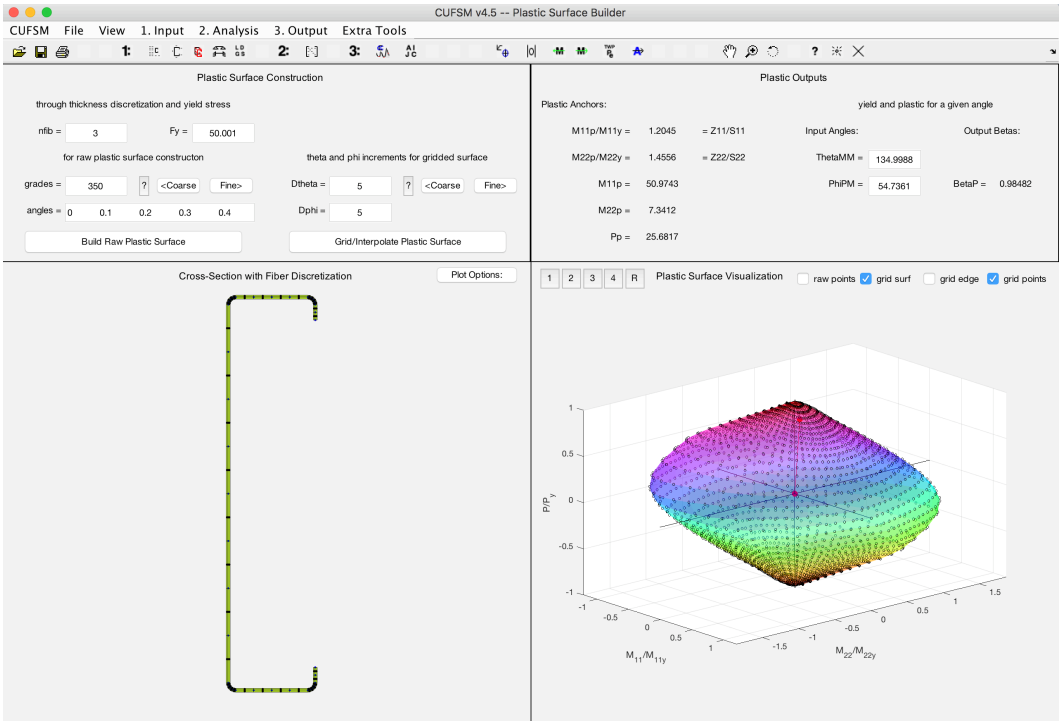

Figure 9: Plastic surface of a lipped channel cross-section (600S137-54) in CUFSM v4.5.

6.2 Plastic Surface

A fiber discretization method is utilized to provide the plastic surface. Fig. 9 shows the plastic surface and the fiber model of a lipped channel cross-section (600S137-54) in CUFSM.

6.3 Elastic Buckling Analysis

Elastic buckling analysis at different length under stress distribution shown in Fig. 8 (first yield stress) leads to the signature curve of the normalized elastic buckling loads. This can be directly determined in the latest version of CUFSM, as shown in Fig. 10.

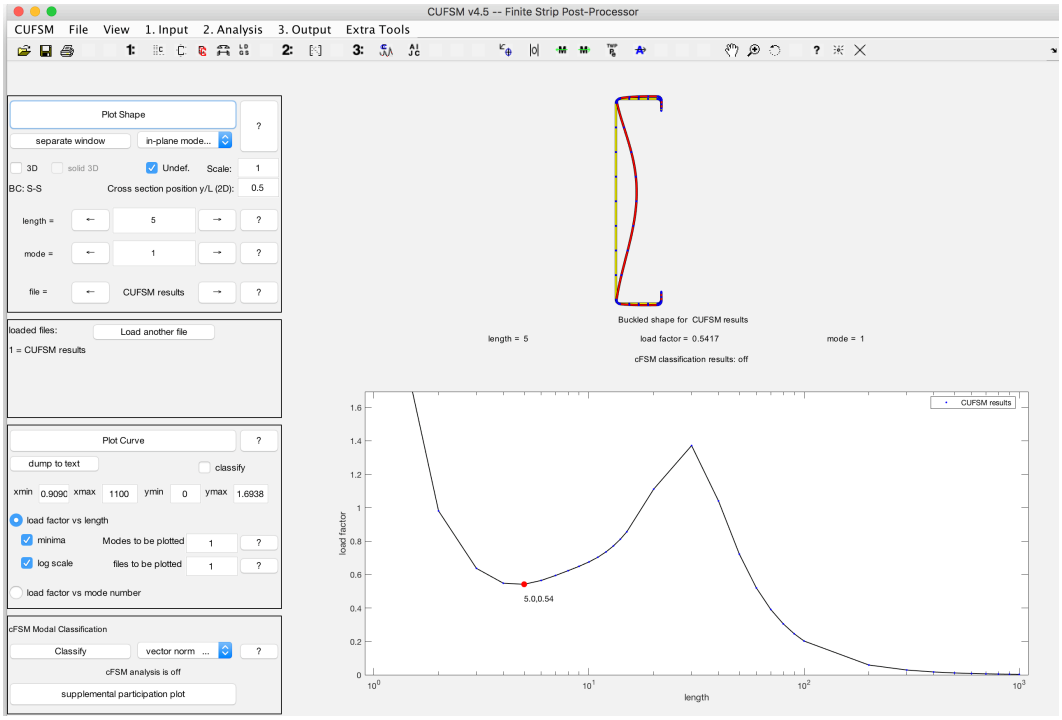

Figure 10: Semi-analytical finite strip method signature curve for 600S137-54 lipped channel at $\theta_{MM}=230^{o}$, and $\phi_{PM}=60^{o}$ in CUFSM v4.5.

7. Conclusions

The development process for the new DSM for cold-formed steel beam-columns is summarized herein. The experimental program and the performed numerical analyses are briefly summarized. A new design expression that directly incorporates stability under the actual applied actions and including inelastic reserve is proposed. Existing experimental studies have been utilized to evaluate the proposed method and reasonable agreement is found between the proposed DSM beam-column predictions and the experimental results. The latest version of CUFSM (v 4.5) that incorporates generalized definition of the demands, yield, and plastic surface modules has been introduced.

Acknowledgments

The authors would like to acknowledge the American Iron and Steel Institute and the Metal Building Manufacturers Association for funding this study. Any opinions, findings, and conclusions or recommendations expressed in this material are those of the authors and do not necessarily reflect the views of the sponsors or other participants.

References

AISI. (2016). *North American specification for the design of cold-formed steel structural members*. American Iron and Steel Institute, Washington, D.C.

Hancock, G. . (2003). "Cold-formed steel structures." *Journal of Constructional Steel Research*, 59(4), 473–487.

Kalyanaraman, V., and Jayabalan, P. (1994). "Local buckling of stiffened and unstiffened elements under nonuniform compression." *International Specialty Conference on Cold-Formed Steel Structures: Recent Research and Developments in Cold-Formed Steel Design and Construction*, 1–9.

Loh, T. S. (1985). "Combined axial load and bending in cold-formed steel members." Ph.D. Thesis, Cornell University, Ithaca, New York.

Macdonald, M., Heiyantuduwa, M. a., and Rhodes, J. (2008). "Recent developments in the design of cold-formed steel members and structures." *Thin-Walled Structures*, 46(7–9), 1047–1053.

Miller, T. H., and Pekoz, T. (1994). "Load-Eccentricity effects on cold-formed steel lipped-channel columns." *Journal of structural engineering*, 120(3), 805–823.

Moen, C. D., Igusa, T., and Schafer, B. W. (2008). "Prediction of residual stresses and strains in cold-formed steel members." *Thin-Walled Structures*, 46(11), 1274–1289.

Pekoz, T. (1986). "Developement of a unified approach to the design of cold-formed steel members." *Eighth International Specialty Conference on Cold-Formed Steel Structures*, St. Louis, MO, 77–84.

Peterman, K. (2012). "Experiments on the Stability of Sheathed Cold-formed Steel Studs Under Axial Load and Bending." (March), 119.

Rondal, J. (2000). "Cold formed steel members and structures: General Report." *Journal of constructional steel research*, 55, 155–158.

Schafer, B. W. (2008). "Review: The Direct Strength Method of cold-formed steel member design." *Journal of Constructional Steel Research*, 64(7–8), 766–778.

Schafer, B. W., and Adany, S. (2006). "Buckling analysis of cold-formed steel members using CUFSM: Conventional and Constrained Finite Strip Methods." *Eighteenth international specialty conference on cold-formed steel structure: University of Missouri-Rolla, Rolla, MO, United States*, Orlando, FL, United States.

Shifferaw, Y. (2010). "Section capacity of cold-formed steel members by the Direct Strength Method." Johns Hopkins University.

Shifferaw, Y., and Schafer, B. W. (2012). "Inelastic Bending Capacity of Cold-Formed Steel Members." *Journal of Structural Engineering*, 138(4), 468–480.

Standards Australia. (2005). *Cold-formed steel structures: NZS 4600*. Standards Australia, Sydney, Australia.

Torabian, S., Amouzegar, H., Tootkaboni, M., and Schafer, B. W. (2016a). "Finite element modeling protocols and parametric analyses for short cold-formed steel zee-section beam-columns." *Annual Stability Conference Structural Stability Research Council, 2016, SSRC 2016*, Orlando, Florida.

Torabian, S., Fratamico, D. C., and Schafer, B. W. (2016b). "Experimental response of cold-formed steel Zee-section beam-columns." *Thin-Walled Structures*, 98, 496–517.

Torabian, S., Zheng, B., and Schafer, B. W. (2014a). "Experimental study and modeling of cold-formed steel lipped channel stub beam-columns." *Proceedings of the Annual Stability*

Conference Structural Stability Research Council, 2014, SSRC 2014, SSRC, Toronto, Canada, 21.

Torabian, S., Zheng, B., and Schafer, B. W. (2014b). "Reliability of the new DSM beam-column design method for cold-formed steel lipped channel." *22nd International Specialty Conference on Cold-Formed Steel Structures, November 2014*, St. Louis, Missouri, USA.

Torabian, S., Zheng, B., and Schafer, B. W. (2015). "Experimental response of cold-formed steel lipped channel beam-columns." *Thin-Walled Structures*, Elsevier, 89, 152–168.

Torabian, S., Zheng, B., Shifferaw, Y., and Schafer, B. W. (2016c). "Direct Strength Prediction of Cold-Formed Steel Beam-Columns." *Reseacrh Report RP16-3, Amerian Iron And Steel Institue*, (October).

Young, B. (2008). "Research on cold-formed steel columns." *Thin-Walled Structures*, 46(7–9), 731–740.

Zeinoddini, V. M., and Schafer, B. W. (2012). "Simulation of geometric imperfections in cold-formed steel members using spectral representation approach." *Thin-Walled Structures*, Elsevier, 60, 105–117.

Zhao, X., Tootkaboni M., Schafer, B.W. (2015). "Laser-based Cross-Section Measurement of Cold-Formed Steel Members: Model Reconstruction and Application". Submitted to Thin-Walled Structures